



HAL
open science

Dynamic Shock Wave-Induced Switchable Phase Transition of Magnesium Sulfate Heptahydrate

Aswathappa Sivakumar, Paramasivam Shailaja, S. Sahaya Jude Dhas, Paramasivam Sivaprakash, Abdulrahman Almansour, Raju Suresh Kumar, Natarajan Arumugam, Sonachalam Arumugam, Shubhadip Chakraborty, S. A. Martin Britto Dhas

► **To cite this version:**

Aswathappa Sivakumar, Paramasivam Shailaja, S. Sahaya Jude Dhas, Paramasivam Sivaprakash, Abdulrahman Almansour, et al.. Dynamic Shock Wave-Induced Switchable Phase Transition of Magnesium Sulfate Heptahydrate. *Crystal Growth & Design*, 2021, 21 (9), pp.5050-5057. <10.1021/acs.cgd.1c00476>. <hal-03367691>

HAL Id: hal-03367691

<https://hal.science/hal-03367691v1>

Submitted on 26 Oct 2021

HAL is a multi-disciplinary open access archive for the deposit and dissemination of scientific research documents, whether they are published or not. The documents may come from teaching and research institutions in France or abroad, or from public or private research centers.

L'archive ouverte pluridisciplinaire **HAL**, est destinée au dépôt et à la diffusion de documents scientifiques de niveau recherche, publiés ou non, émanant des établissements d'enseignement et de recherche français ou étrangers, des laboratoires publics ou privés.



HAL Authorization

1 **Dynamic Shock Waves Induced Switchable Phase Transition of**
2 **Magnesium Sulfate Heptahydrate**

3 Aswathappa Sivakumar¹, Paramasivam Shailaja¹, S.Sahaya Jude Dhas², Paramasivam
4 Sivaprakash³, Abdulrahman I. Almansour⁴, Raju Suresh Kumar⁴, Natarajan Arumugam⁴,
5 Sonachalam Arumugam³, Shubhadip Chakraborty⁵, S.A.Martin Britto Dhas^{1*}

6 ¹Shock Wave Research Laboratory, Department of Physics, Abdul Kalam Research Center,
7 Sacred Heart College, Tirupattur, Tamil Nadu, India – 635 601

8 ²Department of Physics, Kings Engineering College, Sriperumbudur, Chennai, Tamilnadu, India
9 - 602 117

10 ³Centre for High Pressure Research, School of Physics, Bharathidasan University, Tiruchirapalli,
11 Tamilnadu, India- 620 024

12 ⁴Department of Chemistry, College of Science, King Saud University, P.O. Box 2455, Riyadh,
13 Saudi Arabia- 11451

14 ⁵Institut de Physique de Rennes, UMR CNRS 6251, Université de Rennes 1, 35042 Rennes
15 Cedex, France

16 **Corresponding Author:** martinbritto@shctpt.edu

17 **Abstract**

18 To date, even though a large number of shock wave induced irreversible crystal-crystal
19 phase transitions have been reported for the past few decades, switchable phase transitions of
20 solid state materials by dynamic shock waves remain to be quite un-known and also attainment
21 of switchable phase transitions is somewhat a difficult task as compared to the irreversible phase
22 transitions. Hence, experiments on switchable phase transition arising out of materials and the
23 related publications are always considered to be valuable asserts for the materials researchers so
24 as to master over the enhanced understanding of the behavior of materials and their probable
25 applications. Moreover, materials of switchable phase have enormous number of spectacular
26 industrial applications. In the present framework, we have presented and demonstrated the
27 switchable phase transition of magnesium sulfate heptahydrate (MgSO₄.7H₂O) at shocked
28 conditions and the switching behavior has been screened by diffraction, vibrational spectroscopic

29 and optical spectroscopic techniques so as arrive at X-ray diffraction (XRD), Raman scattering
30 and UV-Visible spectral analyses, respectively. All the observed results clearly reveal that the
31 switchable phase transition is achieved at dynamic shock wave loaded conditions. The
32 interesting aspects of the present experimental results with respect to the number of shock pulses
33 are discussed in the upcoming sections.

34 **Key-words:** Magnesium sulfate heptahydrate, Shock waves, Switchable phase transition, Re-
35 crystallization

36 **Introduction**

37 Studies on the impact of shock waves on materials found in the Nature have started to
38 receive a great deal of attention such that their influence on the properties of materials has
39 attained a standpoint of pinnacle which has triggered a series of innovations that have driven
40 efficiency and sustainability of materials to the levels of previously unattainable and this new
41 sphere of activity offers multiple opportunities for the researchers to rise to the occasion.
42 Structured reflection on those lines could provide remarkable scope of finding materials of
43 prominence such that switchable phase transition could be very well established for a few
44 materials by the impact of shock waves. Furthermore, switchable crystallographic phase
45 transition is one of the special topics for materials scientists who work in the crystallographic
46 phase transitions of solids because such materials are highly used in pressure transmitters,
47 molecular switches, current flash memories and phase shifters etc. ¹⁻³ To achieve such special
48 phase transitions, knowledge of the crystal structures at high-pressure, high-temperature and
49 low-temperature environments is highly required. Over the last couple of decades, several
50 thousands of publications have been achieved in the field of static high pressure compression and
51 de-compression enforced on materials such that an array of data have been accomplished through
52 experiments which have paved the way for the switchable phase transitions emerging out of
53 materials as that of solid state phase transitions which include crystal – crystal and crystal –
54 amorphous phase transitions.⁴⁻⁶ It could be noted that, in the case of static high-pressure
55 experiments, many of the materials exhibit such reversibility which has been very well
56 established in both inorganic and organic crystals.⁴⁻⁶ Here we present a few examples of static
57 high-pressure and high-temperature experiments wherein the obtained results of phase transitions

58 in materials could provide convincing substantiation on the above-mentioned statements. Yun-
59 Zhi Tang et al have demonstrated the switchable phase transitions of 18-Crown-6 Clathrate that
60 have been accomplished during the heating and cooling conditions.⁷ Reversible double phase
61 transitions have been observed in Hybrid Iodoplumbate ($C_4H_{12}NPbI_3$) during the process of
62 heating as well as cooling.⁸ Kai Wang et al have performed the static pressure compression and
63 de-compression experiment on sulfamide and found the reversible phase transitions.⁹ Thomas D.
64 Bennett et al have demonstrated the crystal – amorphous reversible phase transitions in zeolitic
65 imidazolate framework at pressure compression and de-compression stages.¹⁰ Bo Zou and his
66 team has performed the static high-pressure experiment and reported the reversible
67 crystallographic phase transition for Ammonium Formate¹¹, Lithium Amide¹², Acetamide¹³ and
68 magnesium silicide (Mg_2Si).¹⁴

69 Followed by the static high-pressure and high-temperature observations analyzed,
70 dynamic shock waves induced phase transition experiments conducted on solids also could
71 provide significant information to the researches to understand the behaviors of molecules and
72 atoms and their response at dynamic high transient pressure and temperature conditions which is
73 identified to be one among the rising research topics in current years.¹⁵⁻¹⁸ It is well known that,
74 during the shock wave loaded conditions, a test sample possibly experiences crystallographic
75 phase transitions of solid to solid^{19,20} and crystal to amorphous phase²¹, lattice deformations and
76 defects^{22,23} and stable crystallographic phase.²⁴ Among the listed three possible occurrences,
77 stable crystallographic phase at dynamic shock wave loaded conditions is quite a rare case to
78 occur since majority of materials experience lots of deformations without undergoing the phase
79 transitions. Furthermore, it is quite interesting to achieve reversible crystallographic phase
80 transitions of solids at shocked conditions as that of static high-pressure experiments. But
81 tremendous amount of effort and energy have been continually paid to achieve such reversible
82 phase transitions in materials at shock wave loaded conditions for the above-mentioned
83 applications since shock wave induced phase transitions are highly rapid than that of the pressure
84 and temperature induced phase transitions. Our research group has reported the switchable
85 crystallographic phase transitions of potassium sulfate crystal at shock wave loaded conditions.²⁵
86 Furthermore, switchable magnetic phase transitions have been observed in $ZnFe_2O_4$ ²⁶ and Co_3O_4
87 NPs.²⁷

88 In the present context, we have chosen magnesium sulfate heptahydrate ($\text{MgSO}_4 \cdot 7\text{H}_2\text{O}$)
89 single crystal to examine the crystallographic phase stability at shocked conditions.
90 $\text{MgSO}_4 \cdot 7\text{H}_2\text{O}$ is one of the familiar polymorphic hydrate salts which is available in the planetary
91 materials.^{28,29} With respect to pressure and temperature, it undergoes series of polymorphic phase
92 transitions based on the prevailing processes of de-hydration and re-hydration.³⁰⁻³² On the one
93 hand, so far, several material scientists and geological scientists have examined the
94 crystallographic phase stability of the title single crystal with respect to pressure, temperature
95 and humidity and have come up with several sequences of phase transitions which are highly
96 associated with the temperature and pressure of the respective experimentation.³⁰⁻³² Moreover,
97 such kinds of high-pressure and high-temperature conditions are highly required to get into the
98 deep understanding of the formation of the present solid state – earth and other planets (Mars and
99 Jupiter) as well as interior icy satellites. On the other hand, through such kind of high-
100 temperature and high-pressure experiments only, we could be able to quantify the water
101 resources of the planets.^{28,29} In recent years, a lot of experiments have been performed on the
102 minerals of Martian planet surface especially magnesium hydrates.^{33,34} Several materials science
103 research groups in the global arena have been continually working on this theme and providing
104 their significant contributions so as to understand better on the phase stability of the title crystal.
105 So far, the known phases of magnesium hydrates are $\text{MgSO}_4 \cdot 11\text{H}_2\text{O}$, $7\text{H}_2\text{O}$ ($\text{P}_{21}2_12_1$), $6\text{H}_2\text{O}$
106 (C_2/C), $5\text{H}_2\text{O}$ (P-1), $4\text{H}_2\text{O}$, $3\text{H}_2\text{O}$, $2\text{H}_2\text{O}$, $1\text{H}_2\text{O}$, and anhydrate MgSO_4 . But, among the listed
107 phases, $\text{MgSO}_4 \cdot 7\text{H}_2\text{O}$ is a thermodynamically stable phase at ambient conditions so that it is one
108 of the promising candidates for heat storage applications due to its high energy density.³⁵⁻³⁷ In
109 some cases, the non-integer water content phase has been observed as that of mixed phase of
110 magnesium hydrate ($\text{MgSO}_4 \cdot 6/7 \text{H}_2\text{O}$) due to the nature of the experiential conditions.³⁵⁻³⁶ In
111 1948, Bridgman has performed high-pressure experiments (piston compression method) on the
112 title crystal and observed a few sluggish phase transitions at 1.0 – 1.5 GPa and 2.5 GPa.³⁸
113 Followed by Bridgmen, Livshits et al have carried out high pressure experiments on crystalline
114 hydrates of magnesium sulfate and found series of phase transitions such as I-II at 0.45 GPa, II-
115 III at 1.2 GPa, III-IV at 1.6 GPa, IV-V at 2.5 GPa.³⁹ Gromnitskaya et al have performed high-
116 pressure neutron powder diffraction study of crystalline $\text{MgSO}_4 \cdot 7\text{H}_2\text{O}$ and found series of phase
117 transitions at 1.4, 1.6, and 2.5 GP.⁴⁰ Very recently, Linfei Yang et al have carried out the

118 combined high-pressure and high-temperature experiments on the title crystal and found three
119 steps of phase transitions with respect to temperature and also observed that the de-hydration rate
120 is increased while increasing the pressure range.⁴¹

121 In the present framework, we have systematically examined the crystallographic phase
122 stability of the title crystal at shocked conditions such that it has been screened by XRD, Raman
123 and UV-DRS techniques. The present shock wave recovery experiments could provide the
124 alternative way to be implemented so as to understand the behaviors of hydrate salts at icy
125 moons and other planets so that it is very much possible to unearth the unknown facts as well as
126 new structural formulations.

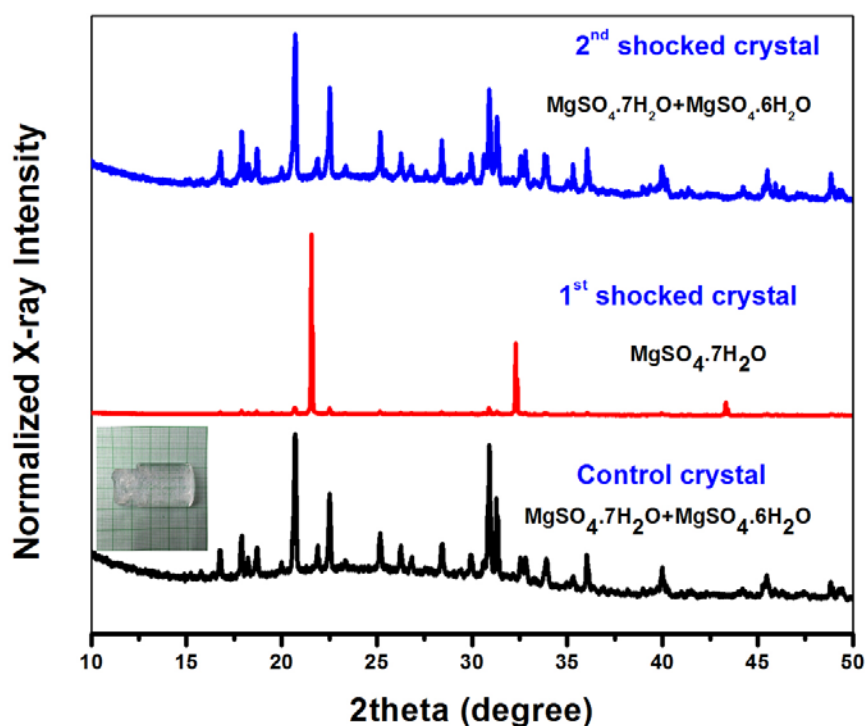
127 **Experimental section**

128 Commercially available, $\text{MgSO}_4 \cdot 7\text{H}_2\text{O}$ was purchased from Sigma Aldrich Company and
129 the material was dissolved in double distilled water. The saturated solution of $\text{MgSO}_4 \cdot 7\text{H}_2\text{O}$ was
130 prepared at room temperature and stirred continuously for 5 hrs with the help of a magnetic
131 stirrer in order to obtain a homogenous solution. Furthermore, the saturated solution was allowed
132 to begin the crystallization process by slow evaporation method and bulk size crystals ($10 \times 10 \times 2$
133 mm^3) were harvested after 25 days so as to be used for the present experiment and the
134 photograph of the as grown crystal is presented in Fig.1 as an inset. The shock wave induced
135 phase stability analysis has been performed using an in-house tabletop semi automatic Reddy
136 Tube for which the details of working methodology have been discussed in our previous
137 papers.^{19,27,42} In the present experiment, we have collected three samples of equal dimension
138 ($5 \times 5 \times 1 \text{ mm}^3$) and have ensured to be defect free crystals so as to be fit for the investigation.
139 Among the three samples, one sample has been kept as the control sample and the remaining two
140 samples have been used for shock wave impact experimentation. In the present experiment, we
141 have used a semiautomatic Reddy Tube for the generation of shock waves of Mach number 2.2
142 possessing transient pressure 2.0 MPa. The crystal is placed in the sample holder such that one
143 shock pulse is exposed on the crystal and two shock pulses are loaded on the other crystal. The
144 time duration between the shock pulses are kept as 5 seconds. After the completion of the shock
145 wave loading procedure, the crystals have been sent for the analytical studies such as XRD,
146 Raman and UV- DRS spectral analyses.

147 **Results and Discussion**

148 **XRD results**

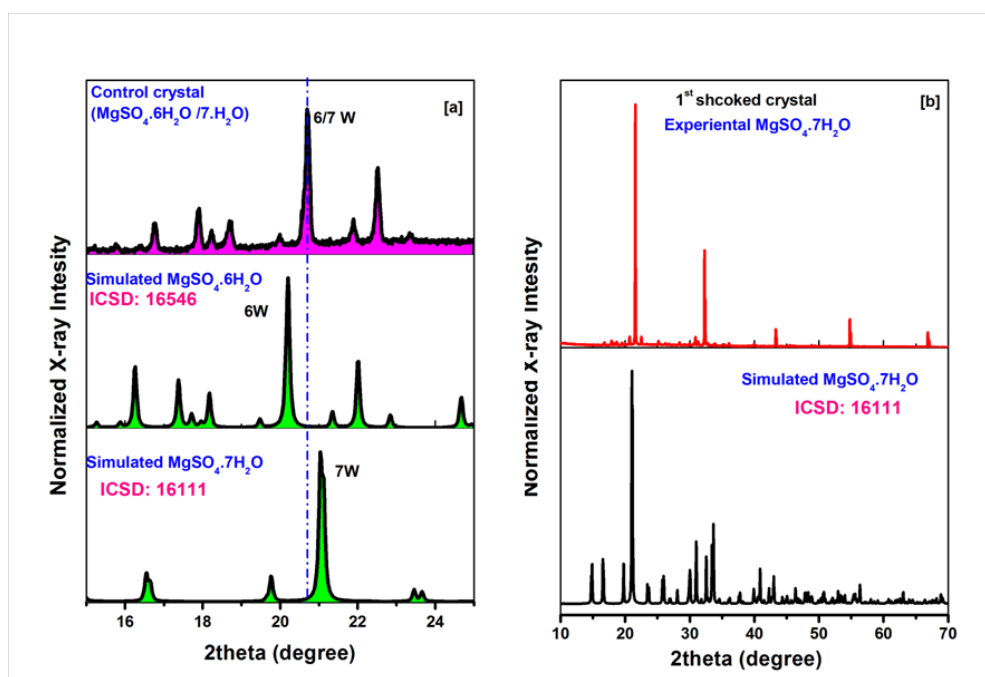
149 Herein, powder X-ray diffractometer has been used for notifying the shock wave induced
150 structural changes of the title crystal and the observed XRD pattern is presented in Fig.1. As per
151 the basic standard, it is quite mandatory to confirm the formation of the crystallographic phase of
152 the test crystal since it is highly sensitive to temperature and pressure. There are enormous
153 possibilities to observe the de-hydration process even at 25-30° C. If such changes occur, the
154 final product structure must be of the lower hydrate phase or mixed phase structure. Hence, the
155 conformation of the grown crystal structure is highly crucial before discussing the shock wave
156 induced changes occurring on the test crystal.



157
158 Fig.1 The XRD patterns of the control and shocked crystals and the photograph of the crystal as
159 an inset

160 The grown crystal's XRD pattern is compared with simulated $MgSO_4 \cdot 7H_2O$ and
161 $MgSO_4 \cdot 6H_2O$ and the corresponding XRD patterns are presented in Fig.2a. As seen in Fig.2a, the

162 prominent diffraction peak position of $\text{MgSO}_4 \cdot 7\text{H}_2\text{O}$ phase is at 21.02 degree and for
 163 $\text{MgSO}_4 \cdot 6\text{H}_2\text{O}$ phase is at 20.01 degree. But in the case of the control crystal (as grown crystal),
 164 the prominent X-ray diffraction peak position is at 20.6 degree and the corresponding XRD
 165 pattern is presented in Fig.2a. Hence, the control test crystal does not belong to a single phase of
 166 $\text{MgSO}_4 \cdot 7\text{H}_2\text{O}$ ($P2_12_12_1$) as well as for $\text{MgSO}_4 \cdot 6\text{H}_2\text{O}$ (C_2/C) so that it is considered as a mixed
 167 phase existing for both the cases. Fig.2a gives the clear justification for the consideration that has
 168 been also witnessed by several researchers i.e. existence of such kinds of mixed phases in
 169 magnesium salts hydrates.^{35,36} There could be two prime reasons for the existence of the mixed
 170 phase for the grown crystal; the first point is, during the de-hydration process occurring at lower
 171 temperature region ($25\text{-}30^\circ\text{C}$), the grains can obviously dehydrate into mixed phases because the
 172 dehydration process is incomplete due to in-sufficient temperature. To achieve complete de-
 173 hydration, it should reach the temperature transition line. As a result, the existing grains do not
 174 have the integer values for the hydrates.^{35,36}

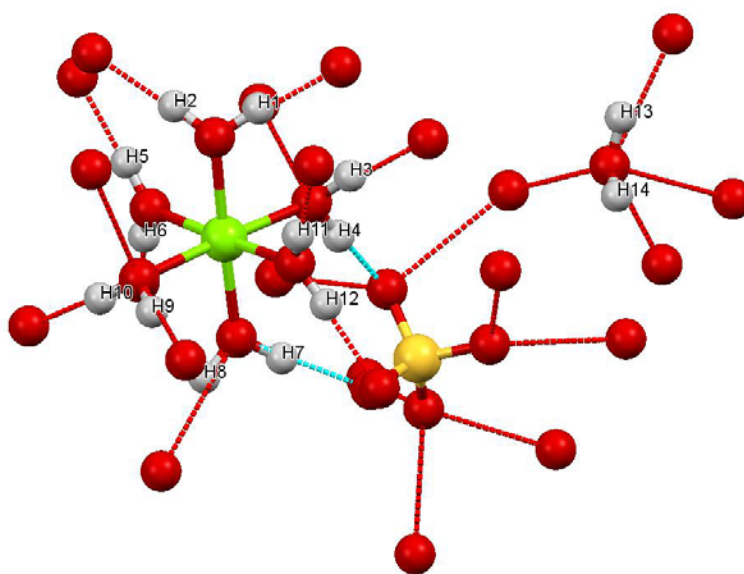


175
 176 Fig.2 (a) Comparison of the XRD patterns of $\text{MgSO}_4 \cdot 7\text{H}_2\text{O}$, $\text{MgSO}_4 \cdot 6\text{H}_2\text{O}$ and the control crystal
 177 (b) The XRD patterns of simulated and shock wave induced $\text{MgSO}_4 \cdot 7\text{H}_2\text{O}$

178 Second point is that some of the lattice waters are changed to pore water states in the
179 same crystal. But, different phases are present due to the in-complete dehydration. Moreover, all
180 the water molecules might not have involved to influence these changes in the crystal.^{35,36} which
181 induces the formation of mixed phases and the observed changes of water states of this crystal
182 will be discussed with reference to the Raman spectroscopic results. As seen in Fig.1, the
183 significant changes have been observed in the XRD pattern with respect to the number of shock
184 pulses. The XRD pattern of the first shocked crystal is completely different from the control
185 sample wherein the most prominent XRD peak is shifted towards the higher diffraction angle
186 which reflects the formation of $\text{MgSO}_4 \cdot 7\text{H}_2\text{O}$. As seen in Fig.2a, the prominent diffraction peak
187 of $\text{MgSO}_4 \cdot 6\text{H}_2\text{O}$ appears at lower diffraction angle as compared to $\text{MgSO}_4 \cdot 7\text{H}_2\text{O}$. But, in the
188 case of 1st shocked condition of the crystal, the prominent XRD peak experiences the higher
189 angle shift and it appears at 21.5 degree. The diffraction value is little larger as compared to the
190 XRD pattern of simulated $\text{MgSO}_4 \cdot 7\text{H}_2\text{O}$. There is no signature for the occurrence of de-
191 hydration process influenced by shock waves even though it has enough transient pressure and
192 temperature. If such de-hydration process has happened, the diffraction peaks would have moved
193 towards the lower diffraction angle and induced the formation of $\text{MgSO}_4 \cdot 6\text{H}_2\text{O}$. But, such kind
194 of reflection is not observed in the XRD pattern of the crystal at 1st shocked condition. Hence, it
195 is very clear that the mixed phase of the test sample is phase transformed to single phase crystal
196 at 1st shocked condition due to the re-organization of hydrogen bonds as well as dynamic re-
197 crystallization. Due to the shock transient pressure and temperature, sufficient latent heat is
198 supplied to the crystal and the extra pore water molecules might be pushed to the lattice water
199 state so that the resultant formation becomes the single phase $\text{Mg} \cdot \text{SO}_4 \cdot 7\text{H}_2\text{O}$. The water
200 molecules are connected with Mg octahedral and SO_4 tetrahedral such that the existing bond
201 pattern is presented in Fig.3. In general, SO_4 tetrahedral is highly sensitive for pressure and
202 temperature and it undergoes significant rotational order-disorder processes at high-pressure and
203 high-temperature conditions.²⁵ Due to the lattice water states changes, the rotational order-
204 disorder of SO_4 tetrahedral is also possible to take place at shocked conditions.²⁵ Due to the
205 existence of the mixed phase during the crystal growth, we can assume in such a way that the
206 disorder SO_4 tetrahedral may be present in the control crystal and specially ordered SO_4
207 tetrahedral appears at 1st shocked condition due to the dynamic re-crystallization which results

208 into single phase $\text{Mg}\cdot\text{SO}_4\cdot 7\text{H}_2\text{O}$ with the $\text{P2}_1\text{2}_1\text{2}_1$ space group. At 2nd shocked condition, the
209 original mixed phase is observed as it is noticed in the control crystal and Fig.1 clearly shows the
210 reversibility of the phases with respect to the number of shock pulses. Hence, at this stage, it is
211 clear that the switchable phase transition is achieved with respect to the number of shock pulses
212 similar to that of K_2SO_4 crystal²⁵ and the schematic diagram of the claimed phase transition is
213 presented in Fig.4.

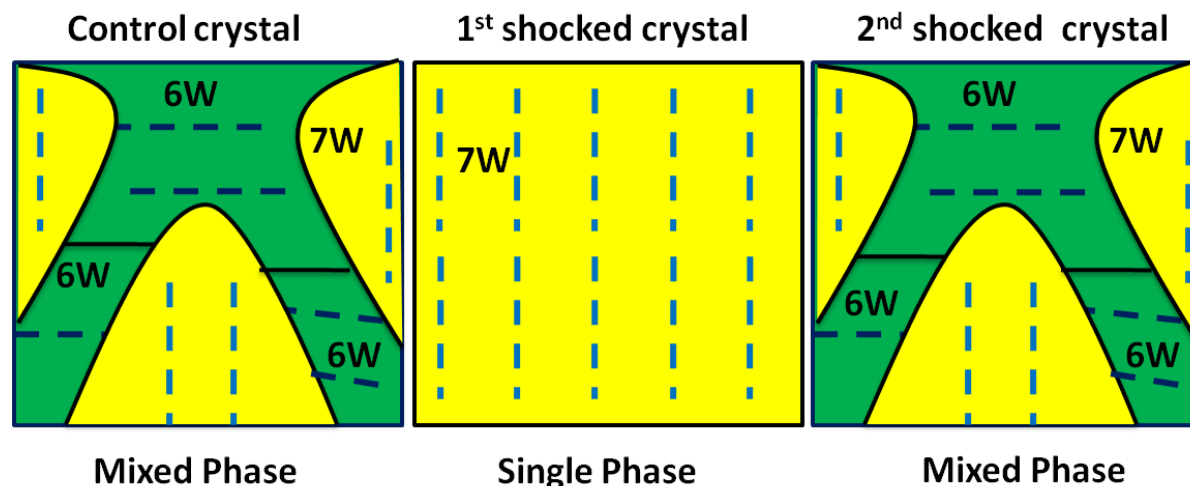
214



215

216

Fig.3 Single molecular bonding pattern of $\text{MgSO}_4\cdot 7\text{H}_2\text{O}$



217

218 Fig.4 Schematic diagram of shock wave induced reversible phase of $\text{MgSO}_4 \cdot 7\text{H}_2\text{O}$

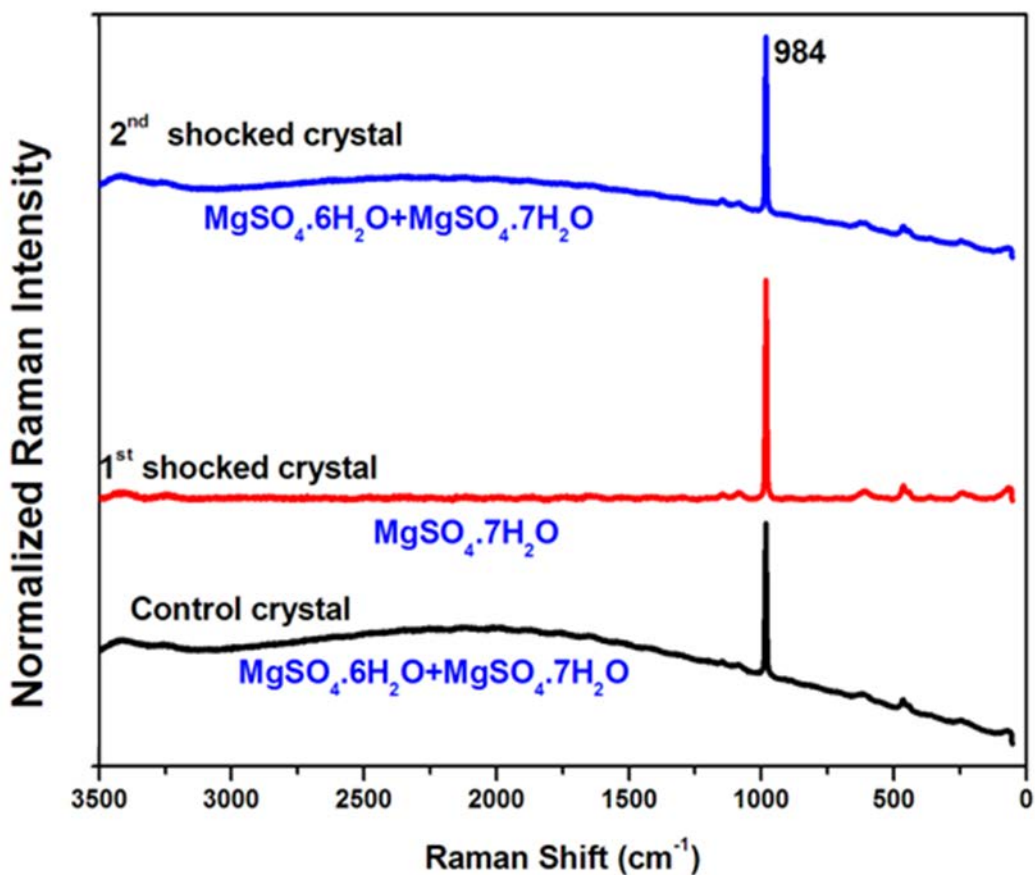
219 During the 2nd shocked condition, some of the lattice water molecules are transferred into
 220 pore water states and as a result the mixed phase is observed. In particular, the seventh water
 221 molecule (H13 and H14 atom in Fig.3) has the maximum possibility to have induced the mixed
 222 phase of $\text{MgSO}_4 \cdot 7\text{H}_2\text{O}$. During the shock wave loaded conditions, the actual $\text{MgSO}_4 \cdot 7\text{H}_2\text{O}$
 223 crystal structure is unable to withstand its own state due to low energy hydrogen bonding
 224 network and try to begin the de-hydration process. Since the existence of the shock wave within
 225 the sample is very short period, the water molecules cannot be able to be removed from the
 226 substance but the seventh water molecule is displaced from its original position where the
 227 hydrogen bond cannot be able to form. Hence the distortion of the crystal structure is highly
 228 possible at shocked condition without the removal of the actual water quantity of the test sample.
 229 In addition to that, the test crystal is a solid substance so that the internal vapor transport is
 230 highly constrained.³⁵ However, the water molecules create a different configuration which leads
 231 to deliquescence and formation of the mixed phase of the crystal. As per the previous reports,
 232 hydrated sulfates undergo dehydration reactions under high temperature and pressure conditions
 233 and result into the formation of lower hydrate structures.^{35,36,40,41} But in the present case, we have
 234 not observed such dehydration process in $\text{MgSO}_4 \cdot 7\text{H}_2\text{O}$.

235

236

237 **Raman Spectroscopic Study**

238 Raman spectroscopic study is one of the powerful techniques to authenticate the
239 molecular fingerprints and solid –state phase transitions of the materials. In the present research
240 work, Raman spectral analysis has been performed so as to justify the XRD results and to
241 understand better the mechanism of the reversible phase transitions of the title crystal such that
242 the observed Raman spectra of the control and shocked crystals are presented in Fig.5.

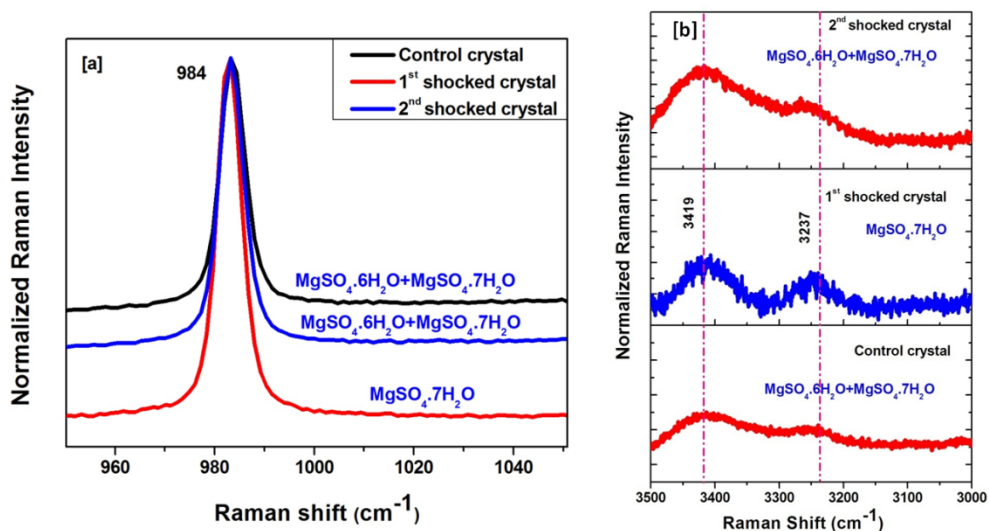


243

244 Fig.5 Raman spectra of the control and shocked crystals

245 As per the previous publications, MgSO₄·7H₂O has the characteristic peaks at 983 cm⁻¹
246 (ν_1 –SO₄), 3322 cm⁻¹ (ν_1 –H₂O) and 3458 cm⁻¹ (ν_3 –H₂O) bands. Based on the XRD results of
247 the present experiment, the control crystal has mixed phase of MgSO₄·7H₂O and MgSO₄·6H₂O
248 such that the observed Raman spectra also justify the XRD results through the vibrational modes

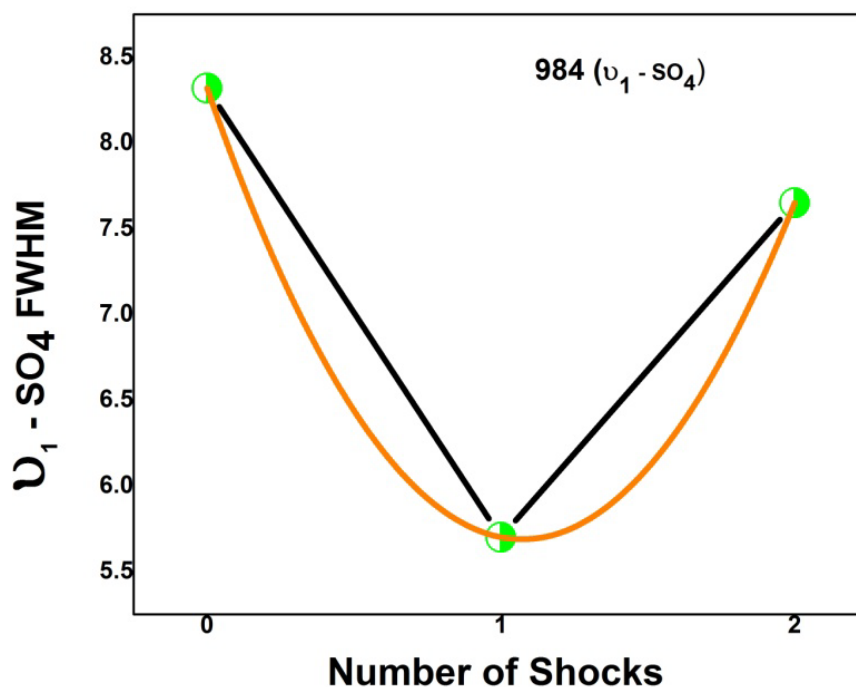
249 of water molecules so that the corresponding zoomed version of the Raman spectra are presented
 250 in Fig.6. The tetrahedral coordination of SO_4 position is almost similar for $\text{MgSO}_4 \cdot 7\text{H}_2\text{O}$ and
 251 $\text{MgSO}_4 \cdot 6\text{H}_2\text{O}$ crystal structures and hence we cannot suspect significant changes in the SO_4
 252 tetrahedral wherein the SO_4 band should move towards the higher wavenumber region during the
 253 de-hydration process expect in $\text{MgSO}_4 \cdot 6\text{H}_2\text{O}$.³⁷ But, in the case of the vibrational modes of water
 254 molecules, one can see considerable changes in the Raman spectra since the lattice water and
 255 pore water transformation has the significant contribution in the formation of the mixed phase.
 256 As seen in Fig.6b, the water molecules identified in Raman bands have less Raman intensity and
 257 high full-width half-maximum (FWHM) values. It may be due to the contribution of the
 258 enhancement of pore water in the crystal than that of the lattice water due to the incomplete de-
 259 hydration process. In addition to that, the strong interaction between lattice water molecules is
 260 reduced during such kinds of incomplete de-hydration process.^{35,36}



261
 262 Fig.6 Zoomed versions of Raman spectra of the control and shocked crystals (a) SO_4 band
 263 (b) H_2O bands

264 So that, the Raman bands of water molecule have less intensity. Followed by the
 265 Raman bands of water molecules, SO_4 tetrahedral Raman band also shows the possible
 266 difference while compared to the pure single phase of $\text{MgSO}_4 \cdot 7\text{H}_2\text{O}$ crystal structure. As seen in
 267 Fig.6a, the control crystal's SO_4 band (984 cm^{-1}) has high full-width half-maximum values
 268 compared to that of $\text{MgSO}_4 \cdot 7\text{H}_2\text{O}$ crystal structure. During the mixed phase formation, the

269 partial $\text{MgSO}_4 \cdot 6\text{H}_2\text{O}$ structure molecules are pulled to the (SO_4) tetrahedral to stay at lower
270 wavenumber side so that the resultant slight changes can be obtained in full-width half-
271 maximum since the actual positions of SO_4 tetrahedral for $\text{MgSO}_4 \cdot 6\text{H}_2\text{O}$ (984.1 cm^{-1}) and
272 $\text{MgSO}_4 \cdot 7\text{H}_2\text{O}$ (984.3 cm^{-1}) crystal structures do not have the great differences.³⁷ At shocked
273 conditions, considerable amount of changes have been noticed in symmetric stretching mode of
274 the sulfate tetrahedral and in the vibrational modes of water molecules. At 1st shocked condition,
275 the SO_4 Raman band showcases less FWHM compared to the control crystal and it is one of the
276 signatures for the existence of the single phase with higher structural order and similar results are
277 also noticed in the XRD results. But the position of the SO_4 Raman band has not changed. On the
278 other hand, highly visible changes have been noticed in the vibrational modes of water molecules
279 both in ($\nu_1 - \text{H}_2\text{O}$) and 3458 cm^{-1} ($\nu_3 - \text{H}_2\text{O}$) bands in particularly their intensities which may be
280 due to the phase transition occurring from mixed phase to single phase of $\text{MgSO}_4 \cdot 7\text{H}_2\text{O}$ crystal
281 structure. The increment of Raman intensity may be due to the transition of some water
282 molecules from pore water states to lattice water states. At this stage, the interaction of lattice
283 water molecules are significantly increased so that strengthening of the hydrogen bonding is
284 increased. Hence, the Raman bands have higher intensity at 1st shocked condition and the
285 obtained phase transitions results are well corroborated with the XRD results. It could be noted
286 that there is no significant dehydration process and formation of pure phase of lower hydrate
287 structures occurred at shocked conditions even though it has enough transient temperature and
288 pressure. At second shocked condition, revert of mixed phase is confirmed due to the existence
289 of the higher value of FWHM for SO_4 (984 cm^{-1}) band water molecules of 3458 cm^{-1} and 3237
290 cm^{-1} . As seen in Fig.6a and b, the band patterns of SO_4 and water molecules are similar. For
291 better understanding of the FWHM values of the control and shocked crystals, we have provided
292 a clear picture about the values with respect to the number of shocks and it is presented in Fig.7.



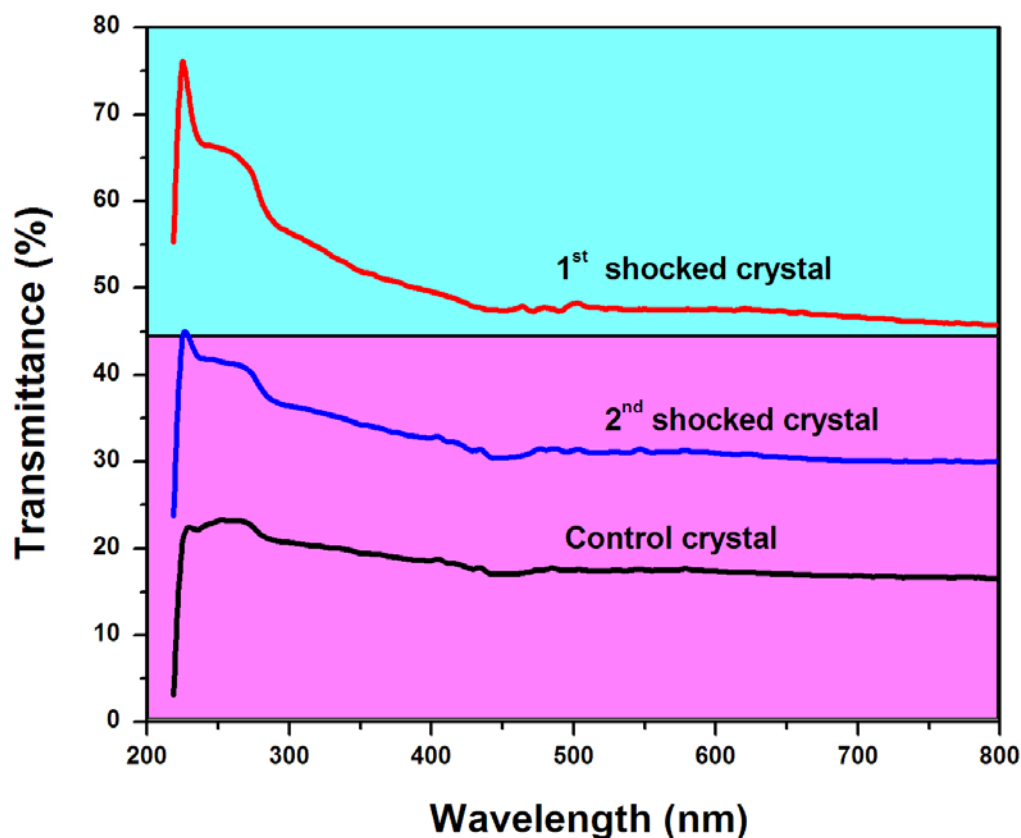
293

294 Fig.7 ν_1 -SO₄ tetrahedral FWHM values of the control and shocked crystals

295 **UV-DRS spectral Analysis**

296 Assessment of optical transmittance for the optically transparent crystals is another
 297 important parameter which can give the possible information to draw the convincing conclusion
 298 about the crystallographic phase transitions.²⁵ Herein, the ultra-violet diffused reflectance
 299 spectrometer (UV-DRS) has been utilized to measure the optical transmittance of the control and
 300 shocked crystal and the observed optical transmittance profiles of the crystal are presented in
 301 Fig.8. As seen in Fig.8, the control mixed phase crystal has transparent window in the entire
 302 visible region. But, the percentage of the optical transmittance is quite low such that the value of
 303 the optical transmittance is 17% at 600 nm. The value is quite convincing even though it is
 304 optically transparent crystal, since the test crystal has the mixed phase it obviously has several
 305 grain boundaries which belong to MgSO₄.7H₂O and MgSO₄.6H₂O. Hence, it is quite obvious
 306 that the net values of the optical transmission are significantly reduced. At first shocked
 307 condition, the optical transmittance spectrum is significantly changed and the value of the optical
 308 transmittance has remarkably increased such that the transmittance value is found to be 47 % at

309 500 nm. This may be due to the formation of single phase $\text{MgSO}_4 \cdot 7\text{H}_2\text{O}$ crystal. At this stage,
310 the light scattering centers are significantly reduced so that the amount of propagation of light
311 has increased giving rise to enhanced optical transmittance.

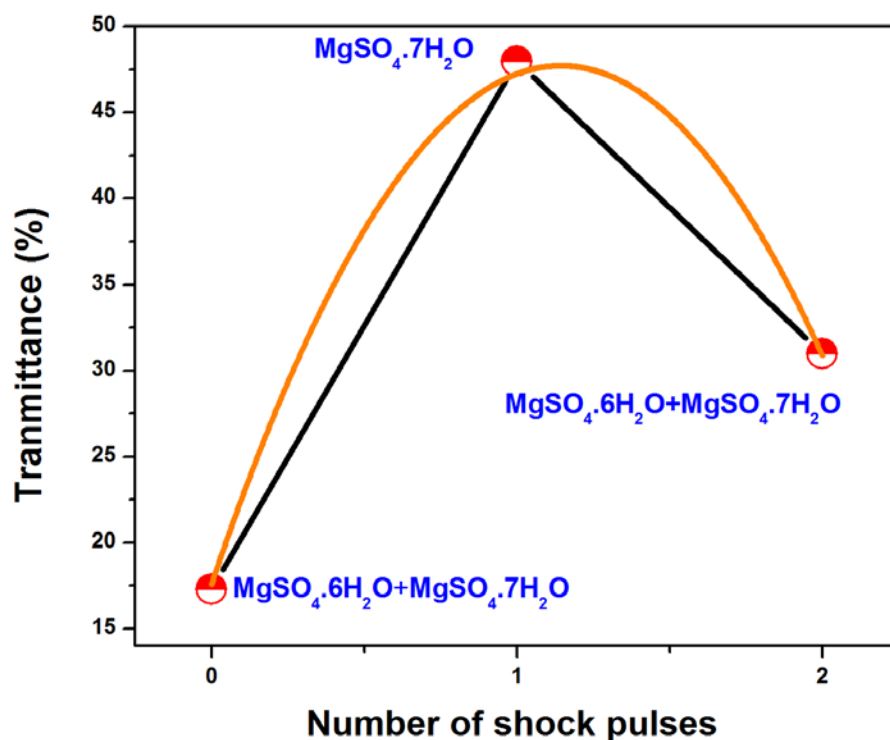


312

313 Fig.8 Optical transmittance spectra of the control and shocked crystals

314 It could be noted that the optical transmittance profile of the 1st shocked crystal is well-
315 matched with the previous reports of $\text{MgSO}_4 \cdot 7\text{H}_2\text{O}$.⁴⁴ At second shocked condition, the
316 percentage of optical transmittance is reduced due to the formation of mixed phase which
317 supports the XRD and Raman results. The optical transmittance percentage of the crystals at 600
318 nm with respect to the numbers of shock pulses is displayed in Fig.9. Based on the optical
319 transmittance analysis, it provides the possible supporting evidence for the observed changes in
320 the XRD and Raman measurement with respect to the number of shock pulses.

321



322

323 Fig.9 The optical transmittance percentage of the control and shocked crystals at 500 nm

324 **Conclusion**

325 In summary, we have systematically demonstrated the switchable phase transitions of
 326 hydrated magnesium salt with respect to the number of shock waves and the results have been
 327 evaluated by XRD, Raman and UV-DRS techniques. The XRD results evidently demonstrate
 328 that the MgSO₄.7H₂O + MgSO₄.6H₂O has been phase transformed to MgSO₄.7H₂O crystal at
 329 the first shocked condition due to the dynamic re-crystallization and changes in the pore water to
 330 lattice water states and the mixed phase is retrieved at the second shocked condition. The Raman
 331 spectral analysis gives the clear picture about the water molecules states which are considerably
 332 changed from pore water states to lattice water states due to the order-disorder process of
 333 tetrahedral (SO₄) with respect to the number of shock pulses and it gives direct correlation for
 334 understanding the switching behavior of the test crystal. UV-DRS spectral analysis also provides
 335 the possible substantiation to justify the XRD and Raman results so that switching of optical
 336 transmittance percentage with respect to the number of shock pulses could also be achieved. It
 337 could be noted that all the three different types of analytical techniques provide the similar

338 authentication with respect to the numbers of shock pulses. Hence, we strongly claim that the test
339 samples have undergone switchable phase transitions and such kinds of materials are highly
340 deserved for applications in sensor, phase shifters, resistive memories and flash memories.
341 Innovative theoretical insights into unlocking the truth behind such shock impacted switching
342 behavior of materials with respect to the number of shock pulses would be extremely valid so
343 that it is reserved for the continual activity which will be in progress for this extended future
344 course of research work. We strongly believe that the present shock wave recovery experiment
345 would provide the new beginning for bringing out many more experiments on hydrate salts of
346 planets so that new structural concepts could emerge at shocked conditions.

347 **Compliance with ethical standards**

348 None

349 **Conflict of interest**

350 The authors declare that they have no conflict of interest.

351 **Acknowledgement**

352 The authors thank Department of Science and Technology (DST), India for funding through
353 DST-FIST programme (SR/FST/College-2017/130 (c)) and for the Abraham Panampara
354 Research Fellowship. The project was supported by Researchers Supporting Project number
355 (RSP-2021/231), King Saud University, Riyadh, Saudi Arabia.

356 **Reference**

- 357 [1] Yi, L.; Hai, T.Z.; Shao-Peng, Chen.; Yu-Hui, T.; Chang-Feng, W.; Chang-Shan, Y.; He, R.
358 W.; Yun-Zhi, T. Reversible Phase Transition and Switchable Dielectric Behaviors
359 Triggered by Rotation and Order-Disorder Motions of Crowns. *Dalton Trans.*, **2018**, *47*,
360 3851-3856.
- 361 [2] Wojciech, W.; and Matthias, W. Reversible switching in phase-change materials.
362 *Mater.Today*, **2008**, *11*, 20-27.
- 363 [3] Yun-Zhi, T.; Yi, L.; Ji-Xing, G.; Chang-Feng, W.; Bin, W.; Yu-Hui, Tan.; and He-Rui,
364 W. Reversible structural phase transition, ferroelectric and switchable dielectric

- 365 properties of an adduct molecule of hexamethylenetetramine ferrocene carboxylic acid.
366 *RSC Adv.* **2017**, *7*, 41369.
- 367 [4] Wen, C.; Mingguang, Y.; Dedi, L.; Quanjun, L.; Ran, L.; Bo, Z.; Tian, C.; and Bingbing,
368 L. Reversible Polymerization in Doped Fullerenes Under Pressure: The Case of
369 $C_{60}(Fe(C_5H_5)_2)_2$. *J. Phys. Chem. B* **2012**, *116*, 2643–2650.
- 370 [5] Yun-Zhi, T., Wang, B.; Hai-Tao, Z.; Shao-Peng, C.; Yu-Hui, T.; Chang-Feng, W.;
371 Chang-Shan, Y., and He-Rui, W. Reversible Phase Transition with Ultralarge
372 Dielectric Relaxation Behaviors in Succinimide Lithium(I) Hybrids. *Inorg. Chem.* **2018**,
373 *57*, 1196–1202.
- 374 [6] Silva, J.A.F.; Freire, P.T.C.; Lima Jr. J.A.; Mendes Filho, J.; Melo, F.E.A.; Moreno,
375 A.J.D.; Polian, A. Raman spectroscopy of monohydrated L-asparagine up to 30 GPa .
376 *Vib. Spectrosc.* **2015**, *77*, 35–39.
- 377 [7] Yun-Zhi, T.; Zhi-Feng, G.; Chang-Shan, Y.; Bin, W.; Yu-Hui, T.; and He, R.W. Unusual
378 Two-step Switchable Dielectric Behaviors and Ferroelastic Phase Transition in a Simple
379 18-Crown-6 Clathrate. *ChemistrySelect*, 2016, *1*, 6772–6776.
- 380 [8] Guangfeng, L.; Jie, L.; Zhihua, S.; Zhenyi, Z.; Lei, C.; Junling, W.; Xutang, T.; and
381 Qichun, Z. Thermally Induced Reversible Double Phase Transitions in an Organic–
382 Inorganic Hybrid Iodoplumbate $C_4H_{12}NPbI_3$ with Symmetry Breaking. *Inorg.*
383 *Chem.* **2016**, *55*, 8025–8030.
- 384 [9] Kai, W.; Jing, L.; Ke, Y.; Bingbing, L.; and Bo, Z. High-Pressure-Induced Reversible
385 Phase Transition in Sulfamide. *J. Phys. Chem. C.* **2014**, *118*, 18640–18645.
- 386 [10] Thomas, D. B.; Petra, S.; Stephen, A. M.; Fabia, G.; Piero, M.; David, A. K.; Jin-Chong,
387 T.; and Anthony, K.C. Reversible pressure-induced amorphization of a zeolitic
388 imidazolate framework (ZIF-4). *Chem. Commun.* **2011**, *47*, 7983–7985.
- 389 [11] Lei, K.; Kai, W.; Shourui, L.; Jing, L.; Ke, Y.; Bingbing, L.; and Bo, Z. Pressure-
390 Induced Phase Transition in Hydrogen-Bonded Supramolecular Structure: Ammonium
391 Formate. *J. Phys. Chem. C.* **2014**, *118*, 8521–8530.
- 392 [12] Xiaoli, H.; Da, L.; Fangfei, L.; Xilian, J.; Shuqing, J.; Wenbo, L.; Xinyi, Y.; Qiang, Z.;
393 Bo, Z.; Qiliang, C.; Bingbing, L.; and Tian, C. Large Volume Collapse during

- 394 Pressure-Induced Phase Transition in Lithium Amide. *J.Phys Chem.C* , **2012**,
395 *116*, 9744–9749.
- 396 [13] Lei, K.; Kai, W.; Shourui, L.; Xiaodong, L.; and Bo, Z. Pressure-Induced Phase
397 Transition in Hydrogen-Bonded Molecular Crystal Acetamide: Combined Raman
398 Scattering and X-ray Diffraction Study. *RSC Adv*, **2015**, *5*, 84703-84710.
- 399 [14] Jian, H.; Bo, Z.; Pinwen, Z.; Chunxiao, G.; Yinwei, L.; Dan, L.; Kai, W.; Weiwei,
400 L.; Qiliang, C.; Guangtian, Z. In situ X-ray observation of phase transitions in Mg₂Si
401 under high pressure. *Solid. State. Commun.* **2009**, *149*, 689–692.
- 402 [15] Sivakumar, A., Saranraj, A.; Sahaya Jude Dhas, S.; Sivaprakash, .P; Arumugam, S.;
403 Martin Britto Dhas, S.A., Spectroscopic assessment on the stability of benzophenone
404 crystals at shock waves loaded condition. *Spectrochim. Acta Part A.* **2020**, *242*, 118725.
- 405 [16] Sivakumar, A.; Suresh, S.; Balachandar, S.; Thirupathy, J.; Kalayana Sundar, J.; Martin
406 Britto Dhas, S.A. Effect of Shock Waves on Thermophysical properties of ADP and
407 KDP crystals. *Optic.Laser.Tech*, **2018**, *111*, 284-289
- 408 [17] Zhi, S.; William, L.S.; Yu-Run, M.; Sizhu, Y.; Dana, D. D.; and Kenneth, S.S. Shock
409 Wave Chemistry in a Metal–Organic Framework. *J.Am.Chem.Soc.* **2017**, *139*, 4619–
410 4622.
- 411 [18] Renganathan , P.; and Gupta. Y. M. Shock compression/release of magnesium single
412 crystals along a low-symmetry orientation: Role of basal slip. *J.Appl.Phys.* **2019**, *126*,
413 115902.
- 414 [19] Kalaiarasi, S.; Sivakumar, A.; Martin Britto Dhas, S.A.; Jose, M., Shock wave induced
415 anatase to rutile TiO₂ phase transition using pressure driven shock tube. *Mater. Lett*
416 **2018**, *219*, 72–75.
- 417 [20] Leiserowitz, L.; and Schmidt, G.M.J. Shock-Induced Irreversible Phase Transitions In
418 Inorganic Solids. *J. Phys. Chem. Solids.* **1966**, *27*, 1453-1457.
- 419 [21] Xuan, Z.; Yu-Run, M.; William, L.S.; Kenneth, S.S.; and Dana D.D. Shock Wave
420 Energy Absorption in Metal–Organic Framework. *J.Am.Chem.Soc.* **2019**, *141*,
421 2220–2223.
- 422 [22] Johannes, R., Shock waves in quasicrystals; *Mater. Sci. Eng*, **2000**, *294*, 753–756.

- 423 [23] Sivakumar, A .; Saranraj, A.; Sahaya Jude Dhas, S.; Jose, M.; and Martin Britto Dhas,
424 S.A., Shock wave-induced defect engineering for investigation on optical properties of
425 triglycine sulfate crystal. *Opt.Eng* **2019**, *58*, 077104.
- 426 [24] Sivakumar, A.; Sahaya Jude Dhas, S.; Martin Britto Dhas, S.A., Assessment of
427 crystallographic and magnetic phase stabilities on MnFe₂O₄ nano crystalline materials at
428 shocked conditions. *Solid State.Sci*, **2020**, *107*,106340.
- 429 [25] Sivakumar, A.; Reena Devi, S.; Sahaya Jude Dhas, S.; Mohan Kumar, R; Kamala
430 Bharathi, K.; and Martin Britto Dhas, S.A. Switchable Phase Transformation
431 (Orthorhombic-Hexagonal) of Potassium Sulfate Single Crystal at Ambient
432 Temperature by Shock Waves. *Cryst. Growth Des.* **2020**, *20*, 7111–7119.
- 433 [26] Mowlika, V.; Sivakumar, A.; Martin Britto Dhas, S. A.; Naveen, C. S.; Phani, A. R. ;
434 Robert, R. Shock wave induced switchable magnetic phase transition behaviour of
435 ZnFe₂O₄ ferrite nanoparticles. *J. Nanostruc.Chem*, **2020**, *10*, 203–209.
- 436 [27] Sivakumar, A.; Soundarya, S.; Sahaya Jude Dhas, S. ; Kamala Bharathi, K. ; and Martin
437 Britto Dhas, S. A., Shock Wave Driven Solid State Phase Transformation of Co₃O₄ to
438 CoO Nanoparticles. *J.Phys.Chem.C* , **2020**, *124*, 10755–10763.
- 439 [28] Alian, W.; Freeman, J. J.; Ming Chou,I.; and Jolliff, B. L. Stability of Mg-sulfates at
440 –10°C and the rates of dehydration/rehydration processes under conditions relevant to
441 Mars. *J.Geophys. Res.* **2011**, *116*, 1-22.
- 442 [29] Alian, W.; Bradley L.J.; Yang, L.; and Kathryn, C. Setting constraints on the nature and
443 origin of the two major hydrous sulfates on Mars: Monohydrated and polyhydrated
444 sulfates. *J. Geophys. Res. Planets*, **2016**, *121*, 678–694.
- 445 [30] Larysa Okhrimenko, Loic Favergeon, Kevyn, Johannes, Frederic Kuznik, Michele
446 Pijolat; Thermodynamic study of MgSO₄ – H₂O system dehydration at low pressure in
447 view of heat storage. *Thermochim. Acta*, **2017**, *656*, 135-143.
- 448 [31] Carolina, C.; Antonio, S.N.; Olmo-Reyes, F.J.; and Daniel Martin Ramos, J. Powder X-
449 ray Thermodiffraction Study of Mirabilite and Epsomite Dehydration. Effects of Direct
450 IR-Irradiation on Samples. *Anal. Chem.* **2007**, *79*, 4455-4462.

- 451 [32] Van Essen, V.M.; Zondag, H.A.; Cot Gores, J.; Bleijendaal, L.P.J.; Bakker, M. ;
452 Schuitema, R.; van Helden, W.G.J. Characterization of MgSO₄ Hydrate for
453 Thermochemical Seasonal Heat Storage. *J. Sol. Energy Eng.* **2009**, *131*, 041014.
- 454 [33] Fortes, A. D.; Wood, I. G.; Vočadlo, L.; Brand, H.E.A.; Grindrod, P.M.; Joy, K. H.; and
455 Tucker, M.G.; The phase behaviour of epsomite (MgSO₄·7H₂O) to 50 kbar: planetary
456 Implications. *Lunar and Planetary Science XXXVII (2006)*
- 457 [34] Grindrod, P.M.; Fortes, A.D.; Wood, I.G.; Sammonds, P.R.; Dobson, D.P.; Middleton,
458 C.A.; and Vočadlo, L., Synthesis and strength of MgSO₄·11H₂O (meridianiite):
459 preliminary results from Uniaxial and triaxial deformation tests. *Lunar and Planetary
460 Science XXXIX (2008)*
- 461 [35] Pim, A.J.D.; Steffen, B.; Leo, P.; Frank, S.; Michael, S.; and Olaf, C.G. A. Water
462 Transport in MgSO₄·7H₂O During Dehydration in View of Thermal Storage.
463 *J.Phys.Chem.C*, **2015**, *119*, 28711–28720.
- 464 [36] Elpida, P.; Luigi, C.; Paolo, B.; Vincenza, B.; Valeria, P.; Angela, C.; Andrea, F.; Luisa,
465 F. C.; Edoardo, P.; and Candida, M.; Morphological and Structural Evaluation of
466 Hydration/Dehydration Stages of MgSO₄ Filled Composite Silicone Foam for
467 Thermal Energy Storage Applications. *Appl. Sci.* **2020**, *10*, 453.
- 468 [37] Kirsten, L.; Michael, N.; Dennis, B.; Konrad, P.; Michael, S. Experimental studies of the
469 mechanism and kinetics of hydration reactions. *Energy Procedia*, **2014**, *48* 394 – 404.
- 470 [38] Bridgman; P. W.; Rough Compressions of 177 Substances to 40,000 Kg/Cm. *Proc. Am.*
471 *Acad. Arts Sci.*, **1948**, *76*, 89-99.
- 472 [39] Livshits, L.D.; Genshaft, Y.S.; Ryabin, Y.N.; Equilibrium diagram of the crystal hydrates
473 of MgSO₄ at high pressures. *Russ. J. Inorg. Chem*, **1963**, *8*, 676–678.
- 474 [40] Gromnitskaya, E. L.; Yagafarov, O. F. Lyapin, A. G.; Brazhkin, V.V.; Wood, I.G.;
475 Tucker, M. G.; Fortes, A. D. The high-pressure phase diagram of synthetic epsomite
476 (MgSO₄·7H₂O and MgSO₄·7D₂O) from ultrasonic and neutron powder diffraction
477 measurements. *Phys Chem Minerals*, **2013**, *40*, 271–285.
- 478 [41] Linfei, Y.; Lidong, D.; Heping, L.; Haiying, H.; Meiling, H.; and Xinyu, Z.; The Phase
479 Transition and Dehydration in Epsomite under High Temperature and High
480 Pressure. *Crystals*, **2020**, *10*, 75.

481 [42] Sivakumar, A.; Balachandar, S.; Martin Britto Dhas, S. A. Measurement of “Shock
482 Wave Parameters” in a Novel Table-Top Shock Tube Using Microphones. *Hum. Fact.
483 Mech. Eng. Defense. Safety.* **2020**, *4*, 3.

484 [43] Bu, C.; Rodriguez Lopez, G.; Dukes, C.A.; Ruesch, O.; Mcfadden, L.A.; and Li, J.Y.,
485 Search for sulfates on the surface of Ceres. *Meteorit Planet Sci*, **2017**, *53*, 1–15.

486 [44] Rathna, N.; Daphne Rebekal, S. Investigations on the Growth, Structural, Optical and
487 SHG Behaviour of Potassium Maesium Sulphate Crystals. *Studies In Indian Place
488 Names*, **2020**, *40*, 3294-3303.

489
490
491
492
493
494
495
496
497
498
499
500
501
502
503

504

For Table of Contents Use Only

505

Dynamic Shock Waves Induced Switchable Phase Transition of

506

Magnesium Sulfate Heptahydrate

507

Aswathappa Sivakumar¹, Paramasivam Shailaja¹, S.Sahaya Jude Dhas², Paramasivam

508

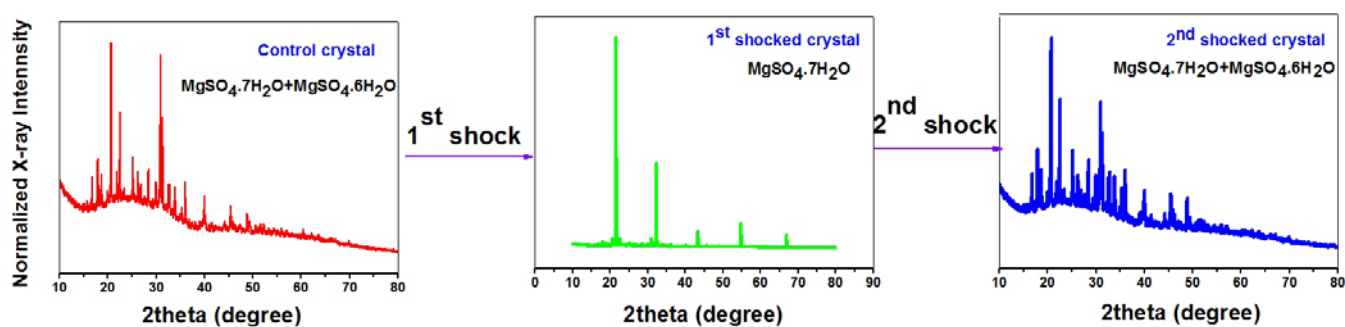
Sivaprakash³, Abdulrahman I. Almansour⁴, Raju Suresh Kumar⁴, Natarajan Arumugam⁴,

509

Sonachalam Arumugam³, Shubhadip Chakraborty⁵, S.A.Martin Britto Dhas^{1*}

510

TOC Graphic Image



511

512

Synopsis

513

Dynamic Shock wave induced reversible phase transformation of $\text{MgSO}_4 \cdot 7\text{H}_2\text{O}$ is achieved at

514

ambient condition due to occurrence of dynamic re-crystallization. The phase transition is

515

evidenced by XRD and Raman spectroscopy.

516

517